JOURNAL OF SOLID STATE CHEMISTRY 91, 271–278 (1991)

EXAFS Study of Lithium-Intercalated Iron Thiophosphate

G. OUVRARD, E. PROUZET, AND R. BREC*

Laboratoire de Chimie des Solides, I.P.C.M., UMR 110, 2 rue de la Houssinière, 44072 Nantes Cedex 03 , France

AND H. DEXPERT

LURE, Batiment 209 D, Université de Paris-Sud, 91405 Orsay Cedex, France

Received July 16, 1990; in revised form October 18, 1990.

The lithium intercalates Li_xFePS_3 ($0 \leq x < 1.5$) were studied using EXAFS at the iron K edge. The important modifications of the spectra were interpreted as originating in displacements of reduced iron atoms from their original octahedral sites to tetrahedral ones. Contrary to parent Li_xNiPS_3 phases where the same cationic shift led to nickel pairs in $(Ni^0S_4)_2$ groups, Fe^0 is found to be located at the same time within the van der Waals gap and within the slab. Although reoxydation of the Li_xFePS_3 phases shift the iron ions to octahedral sites, that of the gap remained partially occupied, the phase undergoing a 2D → 3D structural modification. © 1991 Academic Press, Inc.

I. Introduction

In the two past decades, lithium intercalation in lamellar compounds has been largely studied for possible use in batteries as well as for the characteristics of the hosts after this topotactic reaction. In opposition to most 2D MX_2, the lamellar thiophosphates of general formula MPS_3 (M = first row transition metal at oxidation state II) show, upon lithium intercalation, a rather peculiar behavior: there seems to be no noticeable modification of X-ray powder diffraction patterns and one sees the occurrence of an unusually low oxidation state in the transition metal. To date no intercalated single crystals have been obtained and no complete structural determination on such crystals was done. Because it is difficult to imagine no change at all within the host structure, EXAFS studies have been performed, at the metal K edge, for the lithium-intercalated nickel and iron thiophosphates. This technique is known to be powerful in local structure determination and previous papers (*1*, *2*) revealed the occurrence of important movements of nickel atoms at lithium intercalation and disintercalation. It has been shown that the reduced nickel atoms (at oxidation state 0) move from their initial sulfur octahedral sites to tetrahedral ones in the slab in order to occupy, two by two, adjacent tetrahedra. This process is partially reversible. In the case of the iron derivative $FePS_3$, ^{57}Fe Mössbauer studies on intercalated phases Li_xFePS_3 (*3*) are consistent with the iron reduction from Fe^{2+} to Fe^0. Nevertheless

* To whom correspondence should be addressed.

0022-4596/91 $3.00

this study was based on the hypothesis of an unmodified structure with iron atoms maintaining their octahedral sulfur environment. In this paper the results of an EXAFS study at the iron K edge for various intercalated phases in the series Li_xFePS_3 ($0 \leq x < 1.5$) are described and discussed in comparison with previous studies on nickel and iron derivatives.

II. Materials, Data Acquisition, and Analysis

$FePS_3$ has been obtained by heating the elements in stoichiometric proportions at 700°C in evacuated silica tubes. Lithium intercalation has been performed via the butyllithium technique (*4*) on powders (diameter < 0.1 mm) leading to various phases in the system Li_xFePS_3 with $x = 0.35$, 0.60, 1.11, and 1.41. Previous studies have shown a limit of lithium intercalation at around 1.5 Li per mole of $FePS_3$ followed by a destruction of the host material. In order to study the reversibility of the phenomenon, the higher intercalated phase $Li_{1.41}FePS_3$ was disintercalated to the composition $Li_{0.10}FePS_3$, using an iodine solution in acetonitrile, and then reintercalated to the composition $Li_{1.08}FePS_3$. Lithium content was determined by atomic absorption spectroscopy. Because of their very high sensitivity, the intercalated phases had to be handled in inert atmosphere and conditioned between two adhesive Kapton tapes in an aluminum cell, as described elsewhere (*2*).

The X-ray absorption data were recorded at room temperature at the iron K edge between 6950 and 7950 eV using the synchrotron radiation emitted by the DCI storage ring at LURE. The monochromator was a Si (331) channel cut crystal.

The EXAFS spectra were analyzed using exactly the same procedure as for the analogous nickel phases (*2*). The origin of the energies was taken at 7112.0 eV. The experimental spectra were modeled with the theoretical amplitude and phase shifts calculated by Teo and Lee (*5*), σ and γ values being obtained from the pristine phase $FePS_3$. The fitting procedure of EXAFS spectra was performed in the 50–700 eV range. Due to its very low atomic number and its well known high mobility in such intercalated compounds, the influence of intercalated lithium was considered as very negligible on the EXAFS spectra and was not taken into account in this study. Previous $FePS_3$ single crystal X-ray diffraction structural determinations (*6, 7*) showed an octahedral sulfur coordination of iron with an average iron–sulfur distance of 2.548(5) Å. The second coordination shell of iron is made of three iron atoms at 3.52 Å and six phosphorus atoms at 3.60 Å.

III. Results

The moduli of the Fourier transforms of EXAFS spectra for the studied phases are gathered in Fig. 1. The general behavior seems to be identical to that encountered in the Li_xNiPS_3 system (*2*). As previously observed, besides the first peak in the starting compound, attributed to the sulfur octahedral environment, a new peak appears when lithium is intercalated. The new component, at shorter distances, increases with lithium content at the expense of the starting peak. At the same time, the intensity of the peak corresponding to the second coordination shell decreases with lithium content, but, in a first approximation, more slowly than in the nickel phases.

A. Analysis of the First Coordination Shell

Because Fig. 1 shows a general behavior identical to that observed for the Li_xNiPS_3 series, the same hypothesis of a migration of metal atoms in sulfur tetrahedra was considered when fitting the experimental spectra corresponding to the first coordination

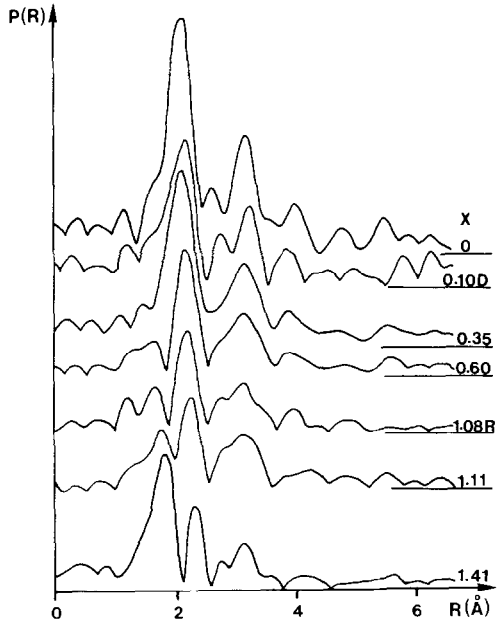

FIG. 1. Moduli of the Fourier transforms of the $k^3\chi(k)$ data at the Fe K edge for various compositions in the Li_xFePS_3 system ($0 \leq x < 1.5$) (uncorrected for phase shift). D and R correspond respectively to the disintercalated and reintercalated phases.

shell. Such an hypothesis is in agreement with the Mössbauer and ESR studies (*3, 8*) which have supported the occurrence of a new type of iron atom upon lithium intercalation. The reasoning already developed for the $NiPS_3$ lithium-intercalated phases (*2*) about the possibility of a site distortion or an off-centered position for the metal atom led us to exclude such an hypothesis. With no evidence of structural modification, the new type of iron was only attributed to the reduced iron atoms remaining in octahedra. Nevertheless these studies concluded unambiguously to a microbiphased process between a reduced phase Li_2FePS_3 and the pristine one, in which iron atoms keep their initial characteristics. This microbiphasing bears out the choice, already made for the nickel phases, to keep constant the σ values for all phases in the Li_xFePS_3 series. This hypothesis allows an improvement in the accuracy of the determination of the numbers of sulfur atoms that correspond to each type of site, and to obtain coherent results for all the family members. Preliminary fits on the starting compound $FePS_3$ led us to determine the value of the electron mean free path ($\gamma = k/\lambda = 2.1$ Å^{-2}), and the σ value at 0.10 Å. During the fits, these values were kept constant and the number of sulfur atoms and the iron–sulfur distance for the two types of sites were allowed to vary with the absorption edge E_0 value.

Table I shows the results of the fits and Fig. 2A compares experimental and calculated signals for the first coordination shell in $Li_{0.60}FePS_3$. The Fe–S distances are fairly constant for all the series, in agreement with the microbiphased process. The mean distance calculated for the first type of site (2.28 Å) is consistent with the value of 2.33 Å encountered, for instance, in Li_2FeS_2 (*9*) where iron is found at oxidation state II in sulfur tetrahedra. It must be pointed out that a larger value was expected for reduced iron atoms but the obtained value agrees well with the one calculated for the reduced nickel atoms in intercalated $NiPS_3$ (2.28 Å). The E_0 variation increases weakly but regularly with lithium content as it does in Li_xNiPS_3.

As suggested by the variations observed

TABLE I

RESULTS OF THE FITS FOR THE FIRST IRON COORDINATION SHELL

x in Li_xFePS_3	$N1$	$R1$(Å)	$N2$	$R2$(Å)	ΔE_0(eV)	r(%)	$X1$	$X2$
0.00			5.9	2.51	14.5	0.40		0.98
0.35	0.6	2.27	5.4	2.51	13.8	0.33	0.15	0.90
0.60	1.0	2.27	3.5	2.52	16.6	0.59	0.25	0.58
1.11	1.6	2.27	2.6	2.51	19.2	3.02	0.40	0.43
1.41	2.7	2.29	1.6	2.51	21.9	1.98	0.67	0.27
0.10 D	0.7	2.29	4.7	2.51	14.9	0.45	0.18	0.78
1.08 R	1.4	2.26	3.1	2.51	15.4	1.75	0.35	0.52

Note. N and R represent respectively the number of sulfur atoms and the Fe–S distances. 1 and 2 refer respectively to tetrahedral and octahedral environment. $X1$ and $X2$ are the fractions of the iron atoms in each type of site ($X1 = N1/4$ and $X2 = N2/6$). ΔE_0 and r represent the edge variation and the reliability factor of the fit.

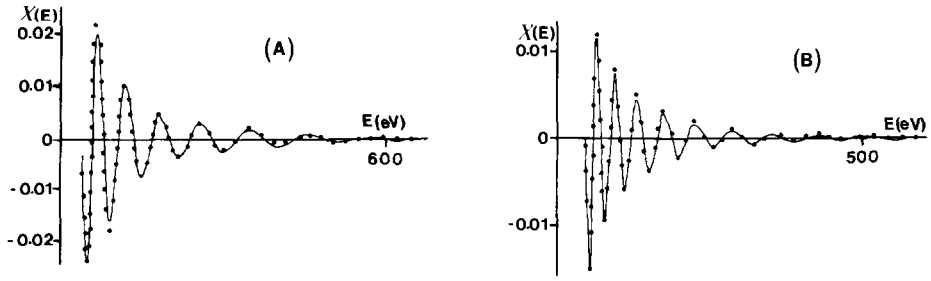

FIG. 2. Some fits between experimental (dots) and calculated (solid lines) signals at the iron edge. (A) First coordination shell for $Li_{0.60}FePS_3$. (B) Second coordination shell for $Li_{1.41}FePS_3$.

in Fig. 1, $N1$ values, which represent the number of sulfur atoms forming the tetrahedra around the iron atoms, increase. At the same time N_2, corresponding to the sulfur octahedra, decreases. From the intercalation–reduction point of view it is more interesting to know the fraction of iron atoms in each type of surrounding. Table I contains $X1$ (equal to $N1/4$) and $X2$ (equal to $N2/6$) values, which represent these fractions for the tetrahedral and octahedral environments, respectively.

B. Analysis of the Second Coordination Shell

Figure 1 shows no occurrence of a new peak in the second coordination shell. From a comparison of EXAFS spectra related to this part of the radial distribution function only the signal intensity seems to be modified but neither the shape nor the frequency. Therefore the fits were performed considering the same atoms (iron and phosphorus) at the same distances for all the series. As for the first coordination shell, the σ values were kept constant. Only the absorption edge position and the number of iron and phosphorus atoms were allowed to vary, leading to very consistent results in the Li_xFePS_3 system. Preliminary fits on $FePS_3$ gave 3.452 and 3.594 Å for Fe–Fe and Fe–P distances, respectively, and 0.105 and 0.135 Å for σ of iron and phosphorus, respectively. These values were kept constant in the following fits. Table II shows the number of iron atoms, N_{Fe}, and phosphorus atoms, N_P, surrounding iron at the above-defined distances and the deduced fractions, $Y1$ (equal to $N_{Fe}/3$) and $Y2$ (equal to $N_P/6$), of iron atoms, keeping the initial cationic environment. Figure 2B compares the experimental and the calculated EXAFS spectra for $Li_{1.41}FePS_3$.

IV. Discussion

Previous Mossbauer studies on Li_xFePS_3 phases and the results obtained on the parent nickel compounds were interpreted as a reduction of metal atoms at the oxidation state zero following a microbiphased process between the starting compound and

TABLE II

RESULTS OF THE FITS FOR THE SECOND IRON COORDINATION SHELL

x in Li_xFePS_3	N_{Fe}	N_P	ΔE_o(eV)	r(%)	$Y1$	$Y2$
0.00	2.9	6.1	10.8	0.26	0.97	1.02
0.35	2.3	5.6	10.6	0.22	0.77	0.93
0.60	1.6	4.7	10.3	0.21	0.53	0.78
1.11	1.3	4.1	9.5	0.19	0.43	0.68
1.41	0.6	3.8	9.8	0.70	0.20	0.63
0.10 D	1.8	3.7	11.2	0.73	0.60	0.62
1.08 R	1.3	3.5	9.7	0.22	0.43	0.58

Note. N_{Fe} and N_P represent the number of iron and phosphorus atoms surrounding absorbing iron. $Y1$ and $Y2$ are the fractions of iron atoms keeping the starting environment deduced respectively from N_{Fe} and N_P ($Y1 = N_{Fe}/3$ and $Y2 = N_P/6$). ΔE_o and r represent the edge variation and the reliability factor of the fit.

the completely reduced phase Li_2MPS_3. In the case of iron phases, such behavior can be written as

$$x\ Li + Fe^{II}PS_3 \rightarrow x/2\ Li^{I}_2Fe^{0}PS_3 + (1 - x/2)\ Fe^{II}PS_3.$$

Figure 3 allows the comparison of the calculated values $X1$ and $X2$, from Table I, and the theoretical fractions of reduced and unreduced domains, from the above reaction, versus x in Li_xFePS_3. Taking into account the low accuracy in the determination of coordination numbers by EXAFS, we can conclude to a good fit between $X1$ values (black circles) and the full line of slope $\frac{1}{2}$ representing the theoretical fraction of reduced phase, and $X2$ values (stars) and the broken line of slope $-\frac{1}{2}$ corresponding to the fraction of unreduced phase. This double agreement indicates a migration of reduced iron atoms from their initial octahedral sulfur sites to tetrahedral ones, as the nickel atoms do in intercalated $NiPS_3$. In this last system, an apparent deficiency of nickel atoms in octahedra was observed and attributed to the simultaneous occupation by reduced nickel atoms of adjacent tetrahedra, constituting of $(NiS_4)_2$ entities. Such a phenomenon is not observed in Fig. 3 and we can conclude to the absence of such Fe–Fe entities in the Li_xFePS_3 intercalates. The apparent nickel deficiency was attributed to an opposition between Ni and S backscattering phases. Almost the same backscattering phases and interatomic distances are found in the iron derivatives and it has been verified that the occurrence of the bimetallic groups should give a decrease in the EXAFS signal in the case of the Li_xFePS_3 series, which is not observed. From the position of $X1$ and $X2$ values of disintercalated and reintercalated phases, it can be concluded to a well reversible process, as far as the first coordination shell is concerned.

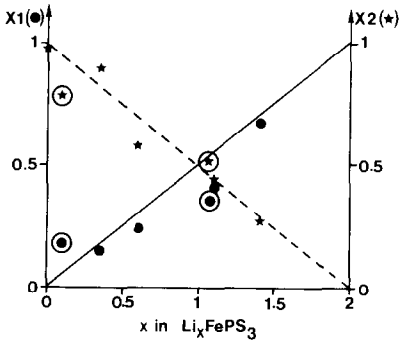

FIG. 3. Fitted fractions of iron atoms in tetrahedral (X1) and octahedral (X2) sulfur sites. The full line and the broken line represent respectively the fraction of reduced and unreduced iron atoms for the hypothesis of a regular reduction from the oxidation state two to zero. The circled values correspond to the disintercalated and reintercalated phases.

This result is not in contradiction with the Mössbauer results (*3*) which were interpreted as a result of an increase of the iron 4*s* orbital population, in order to explain the unusual isomer shift decrease at the intercalation (one would expect the contrary). In fact, it is well known (*10*) that the iron isomer shift is lower, other things being equal, in a tetrahedral environment than in an octahedral one. In Ref. (*3*) it was pointed out that the isomer shift could be due to the geometry change around Fe upon reduction, but there was no strong structural evidence at the time to back up this assumption. Since the iron derivative host structure undergoes an important local modification, it is not possible to perform the same type of calculation based on the assumption of an unaltered structural frame.

The different behavior between iron and nickel derivatives is confirmed by the $Y1$ and $Y2$ variations, versus x in Li_xFePS_3 (Fig. 4). In effect, upon intercalation in $NiPS_3$, $Y1$ and $Y2$ follow rather well the same line of slope $-\frac{1}{2}$, according to a nickel migration in the slab. In Fig. 4, we can observe that, in Li_xFePS_3, if $Y1$ follows rather

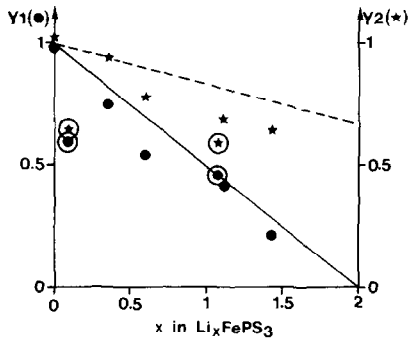

FIG. 4. Fitted fraction of iron atoms keeping the initial second coordination shell calculated either from the number of iron atoms (Y1) or the number of phosphorus atoms (Y2). The full line represents the number of unreduced iron atoms. The broken line corresponds to a theoretical number of phosphorus atoms if all reduced iron atoms occupy the van der Waals gap. The circled values correspond to the disintercalated and reintercalated phases.

well such a line (full line), $Y2$ diverges significantly from it, the data points being located well above. In order to explain these variations, Table III shows the various possible iron environments, for the first and the second coordination shells, considering its four possible situations (tetrahedra or octahedra, in the slab or in the van der Waals gap) and an unmodified general stacking of the polyanionic groups (sulfur and phosphorus atoms unchanged). If only tetrahedra in the slab were occupied, phosphorus atoms would no more be encountered in the second coordination shell but in the first one. Only a migration in the van der Waals gap's tetrahedra can explain the $Y2$ variation, with larger values than the full line. In such a position, iron atoms have four phosphorus atoms at distances not very different from those encountered in the starting compound (3.65 and 3.60 Å, respectively). Should all iron atoms occupy the gap, $Y2$ would follow a variation represented by the broken line (of slope $-\frac{1}{6}$) on Fig. 4. The intermediate position of experimental values between the two theoretical lines seems to favor the assumption of an in-gap and in-slab migration.

This last hypothesis is sustained by the $Y1$ variation. In effect, if we do not consider the presence of iron in adjacent tetrahedra as ruled out above, Table III shows that iron keeps at least two-third's of the initial neighboring iron atoms whether it moves totally in the gap or in the slab in its new tetrahedral site. One possibility or the other is in complete disagreement with the $Y1$ calculated values which indicate that, in

TABLE III

FIRST AND SECOND IRON COORDINATION SHELL VERSUS THE NATURE OF THE SITE OCCUPIED BY IRON IN AN HYPOTHETICAL UNMODIFIED $FePS_3$ STRUCTURE, KEEPING THE PRISTINE POLYANIONIC STACKING

Iron sites	First coordination shell	Second coordination shell
Octahedra in the slab	6 S at 2.55 Å	6 P at 3.60 Å 3 Fe at 3.52 Å
Tetrahedra in the slab	4 S at 2.31 Å 1 P at 2.00 Å 1 P at 2.74 Å	Between 2 and 3 Fe at 3.52 Å (depending on their relative arrangement)
Octahedra in the van der Waals gap	6 S at 2.55 Å	2 P at 2.98 Å 3 Fe at 3.52 Å
Tetrahedra in the van der Waals gap	4 S at 2.31 Å	4 P at 3.65 Å Between 2 and 3 Fe at 3.52 Å (depending on their relative arrangement)

the reduced phase, there are no more iron atoms at starting distances (3.52 Å). In order to agree with the previous conclusions drawn from the *X*1, *X*2, and *Y*2 variations, the only possibility is to consider a distribution of the iron atoms in all the in-slab and in-gap tetrahedra of the structure. In this case, the large number of available tetrahedra (six) per iron atom allows a separation of more than 4 Å between these latter species.

It is worthwhile noticing that such behavior can explain partially the increasing value of the reliability factor for the first coordination shell fits, when the lithium content increases. In effect, as shown in Table III, when iron atoms move within the slab, their first coordination shell contains two phosphorus atoms, at 2.00 and 2.74 Å, not taking into account in the fits.

Finally let us consider the *Y*1 and *Y*2 values for the disintercalated ($Li_{0.10}FePS_3$) and reintercalated ($Li_{1.08}FePS_3$) phases. For the latter the reversibility seems to be rather good. For the disintercalated phase it is very different, with *Y*2 almost unchanged as compared to $Li_{1.41}FePS_3$ and *Y*1 intermediate between the theoretical value and that observed for the more intercalated phase. From Table III, and considering that all iron atoms return to octahedral sites as concluded from the study of the first coordination shell, these results can only be explained by the fact that an important fraction of reoxidized iron atoms are left in the van der Waals gap at the lithium disintercalation. This fraction could correspond to the reduced atoms which have migrated into the gap.

The general behavior of $FePS_3$ upon lithium intercalation can be summarized as follows: (i) migration of reduced iron atoms in tetrahedra of the slab and of the van der Waals gap, in almost equivalent proportions; (ii) return of oxidized iron into octahedra at the disintercalation with the cations remaining in the slab and in the gap. This peculiar behavior explains well the poor performances of lithium batteries built with $FePS_3$ especially in cycling (*11*), the iron atoms left in the van der Waals gap hindering a good lithium diffusion.

V. Conclusion

From previous observations, it could be thought that lithium intercalation in $FePS_3$ would induce the same kind of reduction process as in $NiPS_3$. This is not so, and if the reduction of Fe^{2+} into Fe^0 with a concomittent shift of that species into tetrahedral sites follows the same pattern, the localization of the occupied site by the reduced transition metal is different. In Li_xNiPS_3, all Ni^0 species remain within the host slab and constitute $(NiS_4)_2$ groups with probable Ni–Ni bonds to be related to a particular electronic configuration in relation to the general behaviour of d^{10} cations. In Li_xFePS_3, such metallic groups do not exist, Fe^0 migrating in almost equivalent ratio in tetrahedral positions in the gap and in the slab. Upon oxidation, these metal atoms move to the next octahedral sites, the van der Waals gap being then partially occupied by Fe^{2+}. It is a kind of transformation from two-dimensional to three-dimensional structure, and this probably explains well the poor electrochemical behavior of $FePS_3$ in lithium batteries, as compared to $NiPS_3$, which preserves its low dimensionality.

References

1. G. Ouvrard, E. Prouzet, R. Brec, S. Benazeth, and H. Dexpert, *J. Chim. Phys.* **86,** 1675 (1989).
2. G. Ouvrard, E. Prouzet, R. Brec, S. Benazeth, and H. Dexpert, *J. Solid State Chem.* **86,** 238 (1990).
3. G. A. Fatseas, M. Evain, G. Ouvrard, R. Brec, and M. H. Whangbo, *Phys, Rev. B* **35,** 3082 (1987).

4. M. B. DINES, *Mater. Res. Bull* **10,** 287 (1975).
5. B. K. TEO AND P. A. LEE, *J. Am. Chem. Soc.* **101,** 2815 (1979).
6. W. KLINGEN, G. EULENBERGER, AND H. HAHN, *Z. Anorg. Allg. Chem.* **401,** 97 (1973).
7. G. OUVRARD AND R. BREC, *Mater. Res. Bull.* **20,** 1181 (1985).
8. P. COLOMBET, G. OUVRARD, O. ANTSON, AND R. BREC, *J. Magn. Magn. Mater.* **71,** 100 (1987).
9. L. BLANDEAU, G. OUVRARD, Y. CALAGE, R. BREC, AND J. ROUXEL, *J. Phys. C* **20,** 4271 (1987).
10. J. B. GOODENOUGH AND G. A. FATSEAS *J. Solid State Chem.* **41,** 1 (1982).
11. A. LE MEHAUTE, personal communication.